Cancer Cell
Article

Medulloblastoma Can Be Initiated by Deletion of *Patched* in Lineage-Restricted Progenitors or Stem Cells

Zeng-Jie Yang,[1] Tammy Ellis,[2] Shirley L. Markant,[1] Tracy-Ann Read,[1,3] Jessica D. Kessler,[1] Melissa Bourboulas,[2] Ulrich Schüller,[4] Robert Machold,[5] Gord Fishell,[5] David H. Rowitch,[6] Brandon J. Wainwright,[2,*] and Robert J. Wechsler-Reya[1,*]

[1]Department of Pharmacology and Cancer Biology, Duke University Medical Center, Durham, NC 27710, USA
[2]Institute for Molecular Bioscience, University of Queensland, St Lucia, Brisbane 4072, Australia
[3]Department of Biomedicine, University of Bergen, 5009 Bergen, Norway
[4]Center for Neuropathology and Prion Research, Ludwig-Maximilians-Universität, Feodor-Lynen-Strasse 23, 81377 Munich, Germany
[5]Smilow Neuroscience Program and Department of Cell Biology, NYU School of Medicine, New York, NY 10016, USA
[6]Institute for Regeneration Medicine and Division of Neonatology, UCSF School of Medicine, San Francisco, CA 94143, USA
*Correspondence: b.wainwright@imb.uq.edu.au (B.J.W.), rw.reya@duke.edu (R.J.W.-R.)
DOI 10.1016/j.ccr.2008.07.003

SUMMARY

Medulloblastoma is the most common malignant brain tumor in children, but the cells from which it arises remain unclear. Here we examine the origin of medulloblastoma resulting from mutations in the Sonic hedgehog (Shh) pathway. We show that activation of Shh signaling in neuronal progenitors causes medulloblastoma by 3 months of age. Shh pathway activation in stem cells promotes stem cell proliferation but only causes tumors after commitment to—and expansion of—the neuronal lineage. Notably, tumors initiated in stem cells develop more rapidly than those initiated in progenitors, with all animals succumbing by 3–4 weeks. These studies suggest that medulloblastoma can be initiated in progenitors or stem cells but that Shh-induced tumorigenesis is associated with neuronal lineage commitment.

INTRODUCTION

The cell of origin for most types of cancer remains unknown. Identifying the normal cell that gives rise to a tumor is important because it allows studies of the normal cell to be used as a source of insight into the behavior of the tumor. Moreover, it allows for direct comparisons between tumor cells and their normal counterparts (e.g., using genomic or proteomic approaches) so that key differences and vulnerabilities of tumor cells can be identified. Finally, recent studies suggest that cells resembling the cell of origin may persist in mature tumors and may be critical for propagating these tumors in vivo. If so, identifying the cell of origin may facilitate development of more effective approaches to therapy.

Our studies have focused on the cell of origin for medulloblastoma, a highly malignant tumor of the cerebellum. Medulloblastoma occurs most frequently in children between the ages of 5 and 10 but may occur in adults as well (Ellison, 2002; Packer et al., 1999). Despite important progress in treatment of the disease, the prognosis for many medulloblastoma patients remains bleak: almost half of the patients who develop the disease die from it, and those who survive often suffer severe side effects from the treatment, including cognitive deficits, endocrine disorders, and increased susceptibility to secondary tumors later in life (Heikens et al., 1998; Mulhern et al., 2005; Packer et al., 1999). Improved approaches for treating medulloblastoma are likely to result from a deeper understanding of its molecular and cellular origins.

SIGNIFICANCE

The Sonic hedgehog (Shh) pathway regulates growth of neural progenitors and stem cells, and activation of this pathway has been suggested to play a role in medulloblastoma and other brain tumors. We use conditional *Patched* knockout mice to test the effects of Shh pathway activation in granule neuron precursors and stem cells. We demonstrate that both cell types can serve as cells of origin for medulloblastoma and that the cell in which the tumor is initiated can have an important impact on the rate of tumor progression. Moreover, we show that deletion of *Patched* in stem cells leads to medulloblastoma and not astrocytoma or oligodendroglioma, suggesting that the neuronal lineage may provide a critical context for the oncogenic effects of Shh signaling.

The cell of origin for medulloblastoma has been the subject of debate for many years (Eberhart, 2007; Read et al., 2006). The morphology of tumor cells and their location on the surface of the cerebellum have led to speculation that the tumors arise from granule neuron precursors (GNPs), restricted progenitors that give rise only to granule neurons. In support of this view, immunohistochemical studies have demonstrated that medulloblastoma cells express markers commonly associated with GNPs, such as p75NTR, TrkC, Zic1, and Math1 (Buhren et al., 2000; Pomeroy et al., 1997; Salsano et al., 2004; Yokota et al., 1996). On the other hand, a variety of studies have shown that medulloblastomas can express stem cell markers and can differentiate into both neurons and glia (Hemmati et al., 2003; Singh et al., 2003), raising the possibility that these tumors may arise from multipotent neural stem cells (NSCs). More recently, it has been suggested that some subtypes of medulloblastoma may arise from stem cells and others from GNPs (Gilbertson and Ellison, 2008); however, definitive evidence for the cell of origin of any particular subtype of medulloblastoma remains elusive.

Although analysis of markers expressed by human medulloblastoma cells can provide clues to the cell of origin, such studies have significant limitations. In part, this is because the early stages of tumorigenesis are usually not detectable or accessible in human patients, so inferences about the cell of origin must be made retrospectively based on the phenotype of cells from fully formed tumors. Since these cells may have changed dramatically during the course of tumorigenesis, expression of a particular marker in a tumor cell may not reflect the expression of this marker during development. In these respects, mouse models of medulloblastoma offer significant advantages for studying the origin of the disease.

One of the most powerful and widely studied models of medulloblastoma is the *Patched* (*Ptc*) mutant mouse (Goodrich et al., 1997; Oliver et al., 2005). *Ptc* is an antagonist of the Sonic hedgehog (Shh) signaling pathway, which functions as a critical regulator of both stem cells and progenitors in the central nervous system (Ahn and Joyner, 2005; Balordi and Fishell, 2007; Wechsler-Reya and Scott, 1999). Homozygous *Ptc* knockouts have multiple defects in the neural tube, heart, and other tissues and die early in embryogenesis (Goodrich et al., 1997). Heterozygotes from this strain survive, and approximately 15% of them develop cerebellar tumors that resemble human medulloblastoma (Goodrich et al., 1997; Oliver et al., 2005). Since *Ptc* mutations have also been observed in many human medulloblastomas (Hahn et al., 1996; Johnson et al., 1996; Raffel et al., 1997), these animals have become an important model for the disease. Studies of *Ptc* mutant mice have provided insight into the early stages of tumorigenesis (Oliver et al., 2005), interactions between *Ptc* and other tumor suppressor genes (Hahn et al., 2000; Wetmore et al., 2001; Zindy et al., 2007), and the utility of hedgehog pathway inhibitors as therapeutic agents for medulloblastoma (Romer et al., 2004; Sanchez and Ruiz i Altaba, 2005). However, because *Ptc* is mutated in all cells in these animals (including NSCs and GNPs), they cannot be readily used to study the cell of origin.

To identify the cell of origin for *Ptc*-associated medulloblastoma, we have taken advantage of a conditional allele of *Ptc* (Adolphe et al., 2006; Ellis et al., 2003) that allows inactivation of the gene in either GNPs or NSCs. We show that deletion of *Ptc* in GNPs results in a marked expansion of the external germinal layer (EGL) where granule cells develop. Although many *Ptc*-deficient GNPs eventually stop dividing and differentiate into neurons, in each animal a cohort of GNPs continues to proliferate, and by 3 months of age, all mice develop tumors. Deletion of *Ptc* in multipotent stem cells leads to expansion of the stem cell population, but only stem cells that commit to the granule lineage continue to divide and go on to form tumors. The increased production of GNPs (from the expanded stem cell pool) and the continued growth of these cells during postnatal development leads to rapid tumor formation, with 100% of animals succumbing to medulloblastoma by 3–4 weeks of age. These studies demonstrate that both progenitors and stem cells can respond to Shh signaling and can serve as cells of origin for medulloblastoma.

RESULTS

Math1-cre/Ptc$^{C/C}$ Mice Allow Deletion of *Ptc* in GNPs

Mice heterozygous for mutations in *Ptc* develop cerebellar tumors that resemble human medulloblastoma (Goodrich et al., 1997; Oliver et al., 2005). In these mice, *Ptc* is inactivated in all cells (including GNPs and NSCs), so definitive conclusions about the cell of origin are not possible. To determine whether loss of *Ptc* in GNPs can lead to medulloblastoma, we sought to create GNP-specific *Ptc* knockout mice. To this end, we crossed two strains of mice: *Math1-cre* transgenic mice (Schüller et al., 2007), which express Cre recombinase specifically in GNPs, and conditional *Ptc* knockout (*Ptc$^{C/C}$*) mice (Adolphe et al., 2006; Ellis et al., 2003), which have loxP recombinase recognition sites flanking a portion of the *Ptc* gene.

Math1-cre mice were generated using a construct containing the Cre coding sequence downstream of a 1.4 kb *Math1* enhancer element that has been used previously to express transgenes in GNPs (Machold and Fishell, 2005). To examine expression of Cre protein in these mice, we stained embryonic and postnatal tissues with anti-Cre antibodies (see Figure S1 available online). Consistent with previous studies (Machold and Fishell, 2005; Wang et al., 2005), we found that the Cre protein was first expressed by rhombic lip-derived cells that are destined to leave the cerebellum and give rise to neurons of the deep cerebellar nuclei (DCN) and brainstem (Figure S1A) (Machold and Fishell, 2005). By embryonic day 14.5 (E14.5), Cre was expressed by GNPs in the EGL (Figures S1B–S1D). Cre expression persisted in the EGL for the first 2–3 weeks after birth (Figure S1E); by adulthood, when all GNPs had differentiated into granule neurons and migrated into the internal granule layer (IGL), Cre expression was no longer detectable in the cerebellum (Figure S1F).

To determine whether Cre activity correlated with Cre protein expression, we crossed *Math1-cre* mice with *ROSA26* reporter (*R26R*) mice expressing green fluorescent protein (GFP) preceded by a loxP-flanked stop sequence (Mao et al., 2001). As shown in Figure 1A, neonatal *Math1-cre/R26R-GFP* mice expressed high levels of GFP in the cerebellum. Analysis of postnatal cerebellar sections (Figure 1B) revealed GFP expression only in proliferating GNPs in the outer EGL (Ki67$^+$ cells in Figure 1C) and in postmitotic granule cells in the inner EGL and IGL

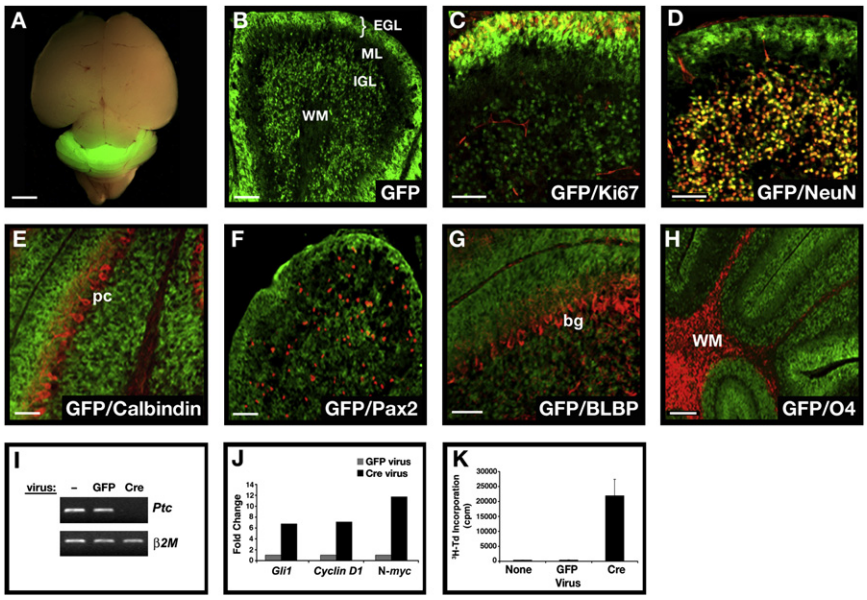

Figure 1. Conditional Knockout Mice Allow GNP-Specific Deletion of *Ptc* and Activation of the Hedgehog Pathway

(A) Brain from P8 *Math1-cre/R26R-GFP* mouse shows Cre-induced GFP expression in the cerebellum.

(B) Cerebellar section shows GFP in the external and internal granule layers (EGL and IGL), but not in the molecular layer (ML) or white matter (WM).

(C and D) Within the EGL and IGL, GFP colocalizes with proliferating (Ki67$^+$) GNPs and postmitotic (NeuN$^+$) GNPs and granule neurons (yellow staining).

(E–H) No GFP is detected in calbindin$^+$ Purkinje cells (pc) (E), Pax2$^+$ interneuron progenitors (F), BLBP$^+$ Bergmann glia (bg) and astrocytes (G), or O4$^+$ oligodendrocytes in the WM (H).

(I and J) GNPs from neonatal $Ptc^{C/C}$ mice were infected with no virus (–) or with viruses carrying *GFP* or *cre-IRES-GFP*. Infected (GFP$^+$) cells were FACS sorted, and mRNA was analyzed by conventional RT-PCR (I) to detect *Ptc* and β2-microglobulin (*β2M*) or by real-time RT-PCR (J) to detect expression of the hedgehog target genes *Gli1*, *Cyclin D1*, and N-*myc*.

(K) Cells infected with the indicated viruses were cultured for 48 hr before being pulsed with tritiated thymidine (^{3}H-Td), cultured for an additional 18 hr, and harvested to measure thymidine incorporation. Data represent means of triplicate samples ± SEM.

Scale bars: 3 mm in (A); 25 μm in (B)–(H).

(NeuN$^+$ cells in Figure 1D). GFP could also be detected in rhombic lip-derived cells that had left the cerebellum and settled in the DCN and brain stem (Figure S2). No GFP was seen in other cell types in the cerebellar cortex, including Purkinje neurons, basket and stellate neurons, Bergmann glia, and oligodendrocytes (Figures 1E–1H). By postnatal day 21 (P21), greater than 95% of NeuN$^+$ cells expressed GFP (Figure S3A), indicating that the majority of granule cells had been exposed to Cre during development. Thus, *Math1-cre* mice can be used to delete loxP-flanked genes in GNPs.

To test the effects of loss of *Ptc* on GNPs, we isolated cells from the cerebellum of neonatal $Ptc^{C/C}$ mice, infected them with Cre-encoding retroviruses, and analyzed expression of *Ptc* and hedgehog target genes by RT-PCR. As shown in Figure 1I, cells infected with *cre* viruses showed no detectable *Ptc* expression. Since Ptc is a negative regulator of the hedgehog pathway (Goodrich et al., 1996), its loss should result in Shh pathway activation. Consistent with this, *cre* retrovirus-mediated deletion of *Ptc* resulted in increased expression of *Gli1*, *Cyclin D1* (*Ccnd1*), and N-*myc*, all previously identified as Shh target genes in GNPs (Kenney et al., 2003; Oliver et al., 2003) (Figure 1J). Finally, Shh pathway activation has been demonstrated to promote proliferation of GNPs (Wechsler-Reya and Scott, 1999); Figure 1K shows that cells infected with *cre* viruses show extensive proliferation compared to cells infected with control viruses. Thus, deletion of *Ptc* in GNPs promotes Shh pathway activation and proliferation.

Deletion of *Ptc* in GNPs Promotes Proliferation but Does Not Prevent Differentiation

We next tested the effects of GNP-specific *Ptc* deletion in vivo by crossing $Ptc^{C/C}$ mice with *Math1-cre* mice. The efficiency of *Ptc* deletion in these mice was examined by laser capturing EGL cells from *Math1-cre*/$Ptc^{C/C}$ cerebella and analyzing their DNA by quantitative PCR; this analysis revealed a >90% reduction in *Ptc* compared to EGL cells from wild-type (WT) mice (Figures S3C and S3D). We then examined the structure of the cerebellum in these animals at various stages of development. At E15, *Math1-cre*/$Ptc^{C/C}$ mice were indistinguishable from WT littermates and showed no significant changes in cerebellar architecture (data not shown). However, after birth (P1–P8), *Math1-cre*/$Ptc^{C/C}$ animals exhibited a dramatic thickening of the EGL (Figures 2E and 2F) compared to WT littermates (Figures 2A and 2B). By P21, all GNPs in WT mice had differentiated and migrated into the IGL, and there was no EGL remaining (Figure 2D). At this stage, the cerebellum of *Math1-cre*/$Ptc^{C/C}$ mice was significantly larger than that of WT littermates (Figures 2C and 2G) and still contained a thick EGL (Figure 2H). These data indicate that deletion of *Ptc* in GNPs leads to severe cerebellar hyperplasia.

Animals with defects in granule cell development often display ataxia or other behavioral abnormalities (Hamre and Goldowitz, 1997; Surmeier et al., 1996). However, at 4–6 weeks of age, most *Math1-cre*/$Ptc^{C/C}$ mice displayed normal behavior, suggesting that at least some normal granule neurons were generated in these animals. To determine whether this was the case, we analyzed the cerebellum of *Math1-cre*/$Ptc^{C/C}$ mice at 6 weeks. In contrast to WT cerebellum (Figures 3A and 3D), the *Math1-cre*/$Ptc^{C/C}$ cerebellum still contained a thick layer of proliferating GNPs on its surface (Figures 3B and 3E). However, beneath this proliferative zone, the normal organization of the cerebellum was maintained, with a distinct Purkinje cell layer surrounding a layer of mature granule neurons that expressed normal differentiation markers (Figure 3E; Figure S4). Deletion of *Ptc* in mature granule cells was confirmed by RT-PCR analysis after laser-capture microdissection (Figures 3G–3I). Some

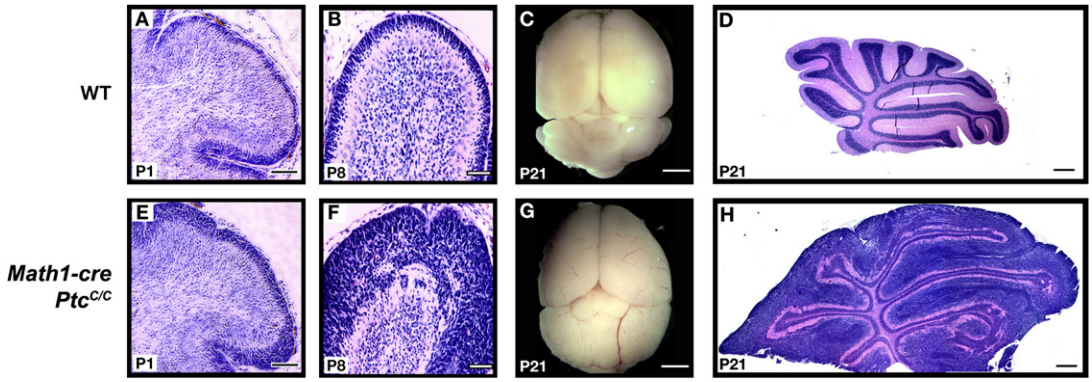

Figure 2. Deletion of *Ptc* in GNPs Leads to Severe Hyperplasia

Math1-cre mice were crossed with $Ptc^{C/C}$ mice, and brains of wild-type (WT) or mutant progeny were harvested at the indicated ages. Brains were fixed and photographed intact (C and G) or sectioned and stained with hematoxylin and eosin (H&E) (A, B, D–F, and H). Note the enlargement of the cerebellum and severe hyperplasia on the surface at P8 and P21. Scale bars: 30 μm in (A), (B), (E), and (F); 2.5 mm in (C) and (G); 400 μm in (D) and (H).

regions of the *Math1-cre*/$Ptc^{C/C}$ cerebellum were more disrupted, showing a nodular structure rather than discrete layers of cells (Figures 3C and 3F). However, even in these regions there was a remarkable conservation of granule cell organization and differentiation, with each nodule containing a core of proliferating GNPs surrounded by a molecular layer, a Purkinje cell layer, and a ring of differentiated granule cells that resembled an IGL (Figure 3F; Figure S4B). These observations suggest that loss of *Ptc* in GNPs results in prolonged proliferation but that many *Ptc*-deficient cells are still able to exit the cell cycle and differentiate into mature neurons.

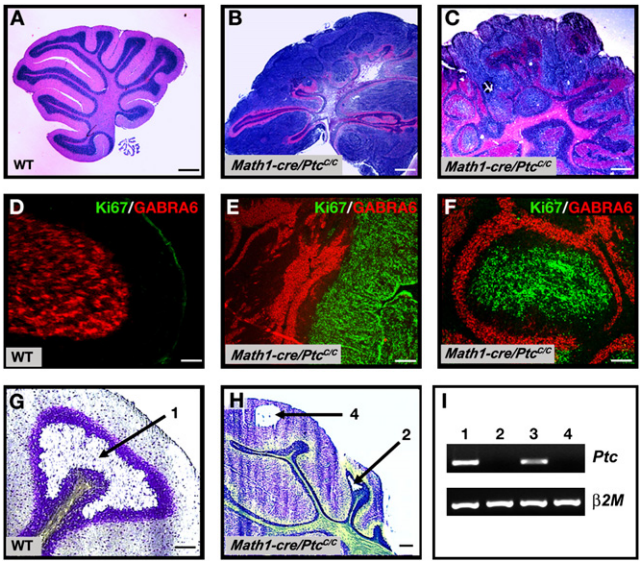

Figure 3. Most *Math1-cre*/$Ptc^{C/C}$ GNPs Differentiate despite Loss of *Ptc*

(A–F) Cerebella from 6-week-old WT (A and D) and *Math1-cre*/$Ptc^{C/C}$ (B, C, E, and F) mice were stained with H&E (A–C) or with anti-Ki67 (green) to detect proliferation and anti-GABRA6 (red) to detect granule neuron differentiation (D–F). Whereas WT cerebella contain no proliferating cells (A and D), mutants exhibit extensive proliferation and differentiation, with proliferating cells either localized to the surface (B and E) or in nodules surrounded by differentiated cells (C and F).

(G and H) Cerebellar sections from 6-week-old WT (G) and *Math1-cre*/$Ptc^{C/C}$ (H) mice were stained with cresyl violet, and the regions indicated by arrows were laser captured for RNA analysis.

(I) RNA from WT IGL (lane 1, derived from region 1 in [G]), *Math1-cre*/$Ptc^{C/C}$ IGL (lane 2, from region 2 in [H]), WT EGL (lane 3, tissue not shown), and proliferating cells at the surface of *Math1-cre*/$Ptc^{C/C}$ cerebellum (lane 4, from region 4 in [H]) were analyzed by RT-PCR for expression of *Ptc* and β2-microglobulin (*β2M*). Note the lack of *Ptc* expression in mutant IGL (lane 2).

Scale bars: 300 μm in (A)–(C); 30 μm in (D)–(H).

Deletion of *Ptc* in GNPs Results in Medulloblastoma

Although *Math1-cre*/$Ptc^{C/C}$ mice were asymptomatic in early adulthood, by 8 weeks of age many animals began to display signs of illness, including domed head, hunched back, abnormal gait, and/or decreased movement. By 10–11 weeks, all *Math1-cre*/$Ptc^{C/C}$ mice became severely ill and had to be sacrificed (Figure 4F). Upon gross examination, the cerebellum from these animals appeared enlarged and covered with blood vessels (Figure 4A). Histological analysis revealed massive tumors that pervaded the cerebellum and obliterated the normal architecture that was present earlier in development (Figure 4B). The tumors could be propagated by transplantation into immunodeficient hosts, indicating that they represented fully transformed tumor cells (Figure 4C). These data suggest that deletion of *Ptc* in *Math1*-expressing cells, while not sufficient to transform every cell, is sufficient to cause tumors in every mouse.

Although *Math1* expression is specific to GNPs in the postnatal cerebellum, during embryonic development the *Math1* enhancer is also expressed in progenitors that end up leaving the cerebellar cortex and migrating to the DCN and brainstem (Machold and Fishell, 2005; Wang et al., 2005) (Figure S2). To determine whether the tumors in *Math1-cre*/$Ptc^{C/C}$ mice could have originated from these progenitors, we crossed $Ptc^{C/C}$ mice with *Math1-creER* transgenic mice (Machold and Fishell, 2005), which express a Cre recombinase-estrogen receptor fusion protein that can be activated by tamoxifen. When *Math1-creER*/$Ptc^{C/C}$ mice were treated with tamoxifen at E10.5—a stage when *Math1* is only expressed by DCN and brainstem progenitors—none of the animals (0/8 mice) developed tumors (Table S1). In contrast, when mice were treated with tamoxifen at E14.5, when *Math1* is expressed in GNPs, 100% of the animals

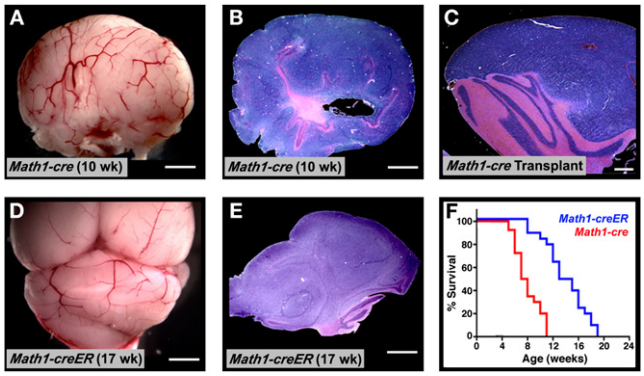

Figure 4. *Ptc* Deletion in GNPs Leads to Medulloblastoma

(A–C) By 10 weeks of age, most *Math1-cre/Ptc*$^{C/C}$ mice develop tumors.

(A) Cerebellum containing tumor.

(B) H&E-stained section of tumor.

(C) H&E-stained section of secondary tumor, induced by transplantation of *Math1-cre/Ptc*$^{C/C}$ tumor cells into cerebellum of adult SCID/beige mouse.

(D and E) Postnatal deletion of *Ptc* in GNPs results in medulloblastoma. *Math1-creER/Ptc*$^{C/C}$ mice were treated with tamoxifen at P4 and sacrificed when symptoms developed (in this case, at 17 weeks). Cerebella were photographed intact (D) or sectioned and stained with H&E (E).

(F) Survival curves for *Math1-cre/Ptc*$^{C/C}$ mice (red) and *Math1-creER/Ptc*$^{C/C}$ mice treated with tamoxifen at P4 (blue).

Scale bars: 3 mm in (A), (B), (D), and (E); 400 μm in (C).

(7/7) developed tumors. These data suggest that tumors in *Math1-cre/Ptc*$^{C/C}$ mice are derived from GNPs.

GNPs are present in mice until 2–3 weeks after birth. To determine whether loss of *Ptc* could trigger medulloblastoma in postnatal GNPs, we treated *Math1-creER/Ptc*$^{C/C}$ mice with tamoxifen at P4 and then examined mice at several time points for changes in cerebellar structure. As with embryonic deletion, postnatal deletion of *Ptc* resulted in increased GNP proliferation and expansion of the EGL by P21 (Figure S5A). GNP proliferation persisted into adulthood, but the majority of *Ptc*-deficient GNPs differentiated and migrated into the IGL, leaving only discrete foci of proliferating cells on the surface of the cerebellum (Figure S5B). By 12 weeks of age, some *Math1-creER/Ptc*$^{C/C}$ animals began to exhibit symptoms of intracranial pressure, and by 19 weeks, all of these mice developed cerebellar tumors (Figures 4D–4F). Tumors were also observed in mice treated with tamoxifen at P8 and P10, but not in animals treated at P12 or later (Table S1). These data indicate that both embryonic and postnatal GNPs can serve as cells of origin for medulloblastoma.

hGFAP-cre/Ptc$^{C/C}$ Mice Allow Deletion of *Ptc* in Neural Stem Cells

Having observed that deletion of *Ptc* in GNPs could cause medulloblastoma, we wondered whether deletion in NSCs would have the same effect. On one hand, since NSCs give rise to GNPs, loss of *Ptc* in these cells might also be expected to result in medulloblastoma. On the other hand, NSCs can also give rise to other types of neurons and glia, so loss of *Ptc* in these cells could potentially lead to other tumor types, such as astrocytoma or oligodendroglioma. To delete *Ptc* in NSCs, we used *hGFAP-cre* mice, in which expression of Cre is controlled by the human glial fibrillary acidic protein (*hGFAP*) promoter (Zhuo et al., 2001). Whereas the *Math1* enhancer drives expression in progenitors after they have left the ventricular zone (VZ) and committed to the granule cell lineage (or are destined for the DCN or brainstem), the *hGFAP* promoter turns on prior to lineage commitment in VZ progenitors that give rise to granule neurons as well as most other types of neurons and glia in the cerebellar cortex (Casper and McCarthy, 2006; Zhuo et al., 2001).

To confirm the specificity of the *hGFAP-cre* transgene, we stained sections from *hGFAP-cre* mice with anti-Cre antibodies at various stages of development and examined expression of GFP in *hGFAP-cre/R26R-GFP* reporter mice. These studies revealed Cre protein expression predominantly in the VZ and in astroglial cells within the cerebellar parenchyma (Figure 5A); no Cre expression was observed in the EGL or in cells expressing *Math1* (Figures S1G–S1L; Figure S6). Nonetheless, analysis of GFP expression in *hGFAP-cre/R26R-GFP* mice indicated that Cre-expressing cells gave rise to granule neurons as well as basket and stellate neurons, Bergmann glia, and oligodendrocytes (Figures 5B–5F; Figure S3B), suggesting that the *hGFAP*$^{+}$ population included multipotent stem cells. Consistent with previous reports (Spassky et al., 2008; Zhuo et al., 2001), no labeling of Purkinje cells was observed, suggesting that these cells arise from a distinct pool of (*hGFAP*$^{-}$) NSCs or are generated at a stage of development prior to expression of the *hGFAP* promoter (Hashimoto and Mikoshiba, 2003).

To confirm that the *hGFAP* promoter is expressed in stem cells, we also isolated GFP^{+} cells from E14.5 *hGFAP-GFP* cerebella (Zhuo et al., 1997) and tested their ability to form neurospheres. FACS-sorted *hGFAP-GFP*$^{+}$ cells generated neurospheres when cultured at clonal density in the presence of growth factors, and individual clones were able to differentiate into neurons, astrocytes, and oligodendrocytes when growth factors were withdrawn (Figure S7). Neurospheres also formed from *hGFAP-GFP*$^{-}$ cells (albeit with 10-fold lower efficiency), suggesting that a subpopulation of embryonic cerebellar stem cells do not express *hGFAP*. These studies indicate that the *hGFAP* promoter is expressed in the majority of NSCs in the embryonic cerebellum and that it can be used to target cells at an earlier stage of differentiation than the *Math1* enhancer.

Deletion of *Ptc* in Stem Cells Results in Medulloblastoma

To examine the consequences of *Ptc* deletion in *hGFAP*-expressing cells, we crossed the *hGFAP-cre* mice with *Ptc*$^{C/C}$ mice and analyzed progeny during embryonic and postnatal development. Between E14.5 and E16.5, *hGFAP-cre/Ptc*$^{C/C}$ mice showed expansion of the VZ, accompanied by increased proliferation and increased expression of group B1 Sox proteins, markers of multipotent stem cells (Figures 6A–6D) (Pevny and Placzek, 2005; Tanaka et al., 2004). Consistent with this, cerebellar cells from *hGFAP-cre/Ptc*$^{C/C}$ mice generated an increased number of neurospheres compared to WT mice (Figure 6E). These neurospheres were able to differentiate into neurons, astrocytes, and oligodendrocytes (Figure S8). Increased neurosphere formation was also observed in *Ptc*$^{C/C}$ cells infected with *cre*-encoding retroviruses in vitro (Figure 6F). Together, these data suggest that *hGFAP-cre*-mediated deletion of *Ptc* results in increased proliferation of NSCs.

During development, NSCs give rise to astrocytes, oligodendrocytes, and several types of neurons. In the *hGFAP-cre/Ptc*$^{C/C}$

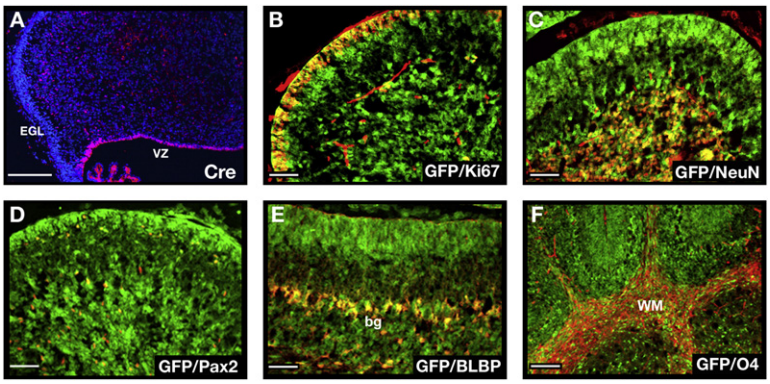

Figure 5. *hGFAP-cre* Mice Express Cre Protein in Neural Stem Cells

(A) Cerebellar sections from E16.5 *hGFAP-cre* mice were stained with anti-Cre antibodies (red) and counterstained with DAPI (blue). Note the expression of Cre in the ventricular zone (VZ) but not in the EGL.

(B–F) Cerebellar sections from P8 *hGFAP-cre/R26R-GFP* mice were stained with anti-GFP antibodies (green) to detect cells that had expressed Cre at some stage of development and with antibodies specific for Ki67 to detect proliferating GNPs (B), NeuN to detect postmitotic granule neurons (C), Pax2 to label interneuron progenitors (D), BLBP to label Bergmann glia (bg) and astrocytes (E), or O4 to detect oligodendrocytes in the white matter (WM) (F). GFP was found to be coexpressed with each of these cell types (yellow staining). Scale bars: 25 μm.

mice, these cells should all lack *Ptc*, since they arise from *Ptc*-deficient NSCs. Despite this, no obvious abnormalities were seen in astrocytes, oligodendrocytes, or non-granule neurons of *hGFAP-cre/Ptc*$^{C/C}$ mice (data not shown). In contrast, marked changes were seen in VZ-derived cells that migrated to the rhombic lip and committed to the granule lineage. *hGFAP-cre/Ptc*$^{C/C}$ mice exhibited a dramatic expansion of the rhombic lip and EGL at E16.5 (Figures 7A and 7B). After birth, when the WT cerebellum contained only one to two rows of GNPs on its surface, the *hGFAP-cre/Ptc*$^{C/C}$ cerebellum was encompassed by a thick, disorganized EGL (Figures 7C and 7D). Analysis of genomic *Ptc* from the postnatal EGL confirmed that there was near complete (>90%) deletion of *Ptc* at this stage (Figures S3C and S3D). By P14, the entire cerebellum was filled with GNP-like cells, and animals began to show symptoms of illness (Figures 7E and 7F). By 4 weeks, all *hGFAP-cre/Ptc*$^{C/C}$ mice developed cerebellar tumors and were sacrificed (Figures 7G–7I). These data show that tumors can be induced by deletion of *Ptc* in multipotent progenitors as well as in lineage-restricted GNPs.

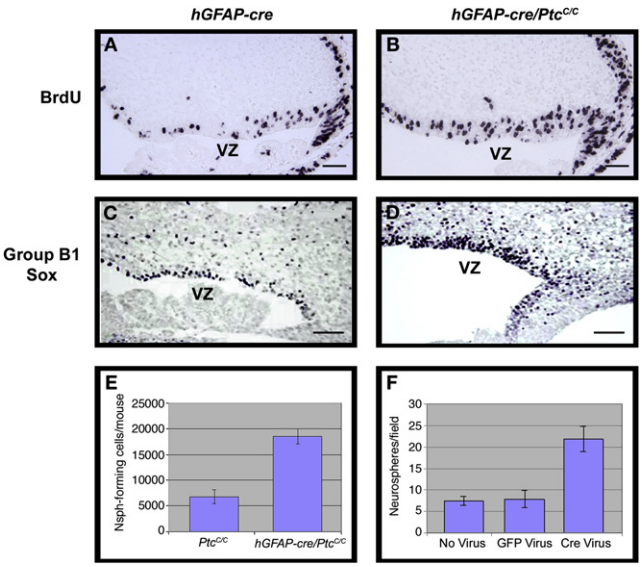

Figure 6. *hGFAP-cre*-Mediated Deletion of *Ptc* Leads to Expansion of NSCs

(A–D) *hGFAP-cre* (A and C) and *hGFAP-cre/Ptc*$^{C/C}$ (B and D) embryos were pulsed with BrdU 2 hr before being sacrificed at E14.5. Brains were harvested, and cerebellar sections were stained with anti-BrdU (A and B) or anti-group B1 Sox (C and D) antibodies. Cerebella from *hGFAP-cre/Ptc*$^{C/C}$ mice contained significantly more BrdU^{+} and SoxB1^{+} cells in the ventricular zone (VZ). Scale bars: 20 μm.

(E and F) Deletion of *Ptc* in embryonic cerebellar cells promotes increased neurosphere formation. Data represent means of triplicate samples ± SEM.

(E) Cerebella from E14.5 *Ptc*$^{C/C}$ and *hGFAP-cre/Ptc*$^{C/C}$ embryos were dissociated, and cells were cultured at clonal density in neurosphere medium. The number of neurospheres per mouse was calculated by multiplying the number of cells obtained from each embryo by the number of neurospheres observed in cultures from that embryo. Cerebella from *hGFAP-cre/Ptc*$^{C/C}$ mice yielded 2.7 times more neurospheres than those from *Ptc*$^{C/C}$ mice.

(F) Cells isolated from E14.5 *Ptc*$^{C/C}$ embryos were infected with no virus or with viruses carrying GFP or *cre-IRES-GFP*. Infected (GFP^{+}) cells were sorted and cultured at clonal density in neurosphere medium. After 7 days, *cre* virus-infected cells generated 2.8 times more neurospheres than GFP-infected cells and noninfected cells.

Interestingly, tumors in *Math1-cre/Ptc*$^{C/C}$ mice and *hGFAP-cre/Ptc*$^{C/C}$ mice expressed abundant and comparable levels of the GNP marker *Math1* and the proliferation marker Ki67 (Figures 8A–8D). In regions of differentiation, most cells expressed the neuronal differentiation markers NeuN, synaptophysin, and GABRA6 (Figures 8E and 8F; data not shown). Few tumor cells in either strain expressed markers of neural stem cells, non-granule neurons, or glia, and cells that did express these markers were almost never proliferative (Figures 8G–8J). Tumor cells from *hGFAP-cre/Ptc*$^{C/C}$ mice and *Math1-cre/Ptc*$^{C/C}$ mice also exhibited similar levels of proliferation (Figure 8K) and induced tumors with similar efficiency and latency following transplantation of 0.05–1.0 × 10^{6} tumor cells into immunodeficient hosts (Figure 8L; data not shown). These observations indicate that tumors initiated in stem cells and progenitors are remarkably similar. The dramatic expansion of the EGL in neonatal *hGFAP-cre/Ptc*$^{C/C}$ mice and the predominant expression of GNP markers in tumors from both strains suggest that tumor formation in these animals is restricted to the granule lineage. Thus, medulloblastoma can be initiated by deletion of *Ptc* in multipotent stem cells or lineage-restricted progenitors, but the oncogenic effects of Shh signaling are only manifest once cells have committed to the granule lineage.

DISCUSSION

The origin of medulloblastoma has been the subject of controversy for many years (Eberhart, 2007; Read et al., 2006). Although some investigators have speculated that these tumors

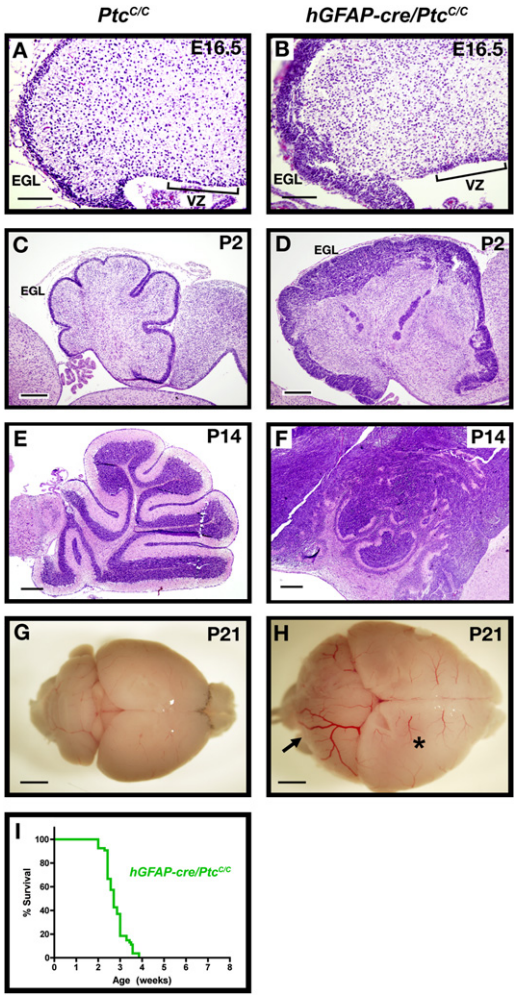

Figure 7. Deletion of *Ptc* in NSCs Results in Rapid Tumor Formation

(A–H) Cerebellar sections from $Ptc^{C/C}$ (A, C, E, and G) and *hGFAP-cre*/$Ptc^{C/C}$ (B, D, F, and H) mice were harvested and stained with H&E (A–F) or photographed whole-mount (G and H) at E16.5–P21. Note the expansion of both the VZ and EGL at E16.5 (A and B) and the persistent expansion of the EGL at postnatal ages (C–F). The arrow in (H) points to a tumor that has formed in the cerebellum. The forebrain (asterisk in H) in these animals also appears enlarged; histological examination (not shown) indicates that this is due to expansion of the ventricle (perhaps due to occlusion of cerebrospinal fluid circulation) rather than to increased growth or tumorigenesis in the cortex.

(I) Survival curve for *hGFAP-cre*/$Ptc^{C/C}$ mice.

Scale bars: 20 μm in (A) and (B); 100 μm in (C) and (D); 300 μm in (E) and (F); 2.5 mm in (G) and (H).

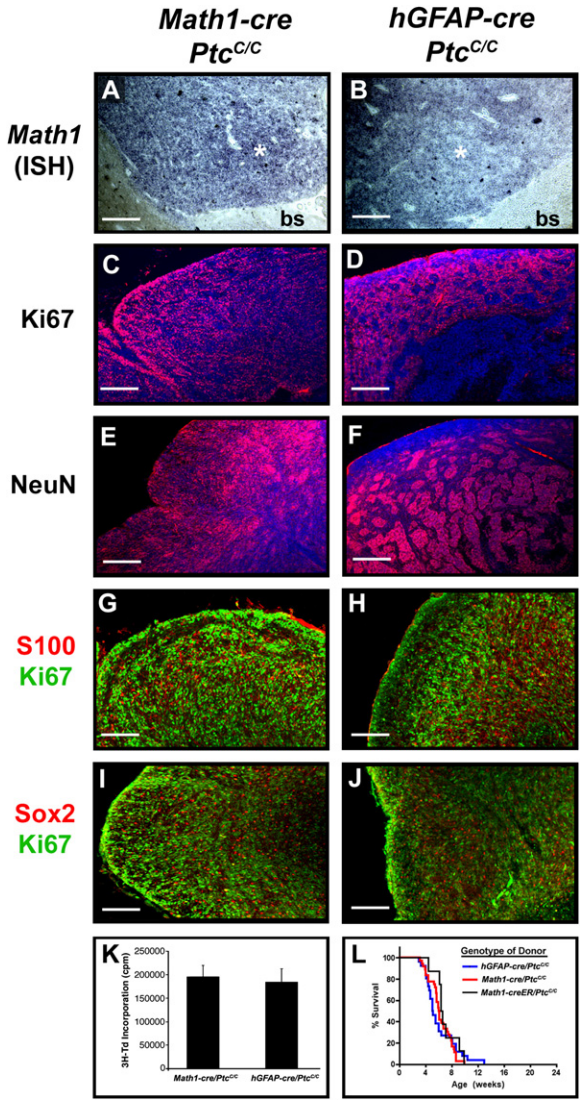

Figure 8. Tumors from *Math1-cre*/$Ptc^{C/C}$ and *hGFAP-cre*/$Ptc^{C/C}$ Mice Display Similar Phenotypes

(A–J) Sections from *Math1-cre*/$Ptc^{C/C}$ (A, C, E, G, and I) and *hGFAP-cre*/$Ptc^{C/C}$ (B, D, F, H, and J) tumors were subjected to in situ hybridization to detect expression of *Math1* (A and B) or stained with antibodies to detect proliferating cells (Ki67; C, D, G, H, I, and J), differentiating neurons (NeuN; E and F), astrocytes (S100; G and H), and stem cells (Sox2; I and J). Sections in (C)–(F) were counterstained with DAPI (blue). In (A) and (B), asterisk denotes tumor and "bs" indicates brainstem. Scale bars: 25 μm.

(K) Tumor cells were cultured for 48 hr, pulsed with tritiated thymidine (^{3}H-Td), and harvested 18 hr later for measurement of thymidine incorporation. Data represent means of triplicate samples ± SEM.

(L) Survival curves of SCID/beige mice after transplantation of 1 × 10^6 tumor cells isolated from *hGFAP-cre*/$Ptc^{C/C}$ mice, *Math1-cre*/$Ptc^{C/C}$ mice, and *Math1-creER*/$Ptc^{C/C}$ mice that had been treated with tamoxifen at P4.

arise from GNPs, the evidence has been largely circumstantial: the morphology of tumor cells, the location of these cells on the surface of the cerebellum (where GNPs develop), and the expression of GNP-associated markers. The fact that Shh is mitogenic for GNPs (Wechsler-Reya and Scott, 1999) and the observation that medulloblastomas in $Ptc^{+/-}$ mice resemble GNPs (Goodrich et al., 1997; Oliver et al., 2005) have suggested that *Ptc*-associated tumors in particular might be derived from these cells. However, the recent observations that Shh is required for stem cell growth and maintenance (Ahn and Joyner, 2005; Balordi and Fishell, 2007) and that medulloblastomas often express stem cell markers (Hemmati et al., 2003; Singh et al., 2003) have cast doubt on this view. By deleting *Ptc* in GNPs and in stem cells, we provide direct evidence that each of these cells can serve as a cell of origin for Shh pathway-associated medulloblastoma.

Tumorigenesis is thought to depend on a capacity for long-term self-renewal. During normal development, GNPs do not exhibit this capacity: they proliferate for 2–3 weeks after birth and then exit the cell cycle and undergo terminal differentiation. The fact that GNPs in *Math1-cre*/$Ptc^{C/C}$ mice continue to proliferate into adulthood (and continue to divide following transplantation) suggests that loss of *Ptc* can increase the self-renewal capacity of these cells. Thus, while neural stem cells—which are thought to have an intrinsic capacity for long-term self-renewal—might represent a good target for oncogenic transformation, restricted progenitors can also become transformed if, through mutation, they acquire the capacity for long-term self-renewal. The ability of oncogenic mutations to increase the self-renewal capacity of lineage-restricted progenitors has also been demonstrated in the hematopoietic system (Cozzio et al., 2003; Krivtsov et al., 2006).

Our studies show that deletion of *Ptc* in GNPs promotes a dramatic increase in proliferation of these cells and results in tumors in all mice. However, it is notable that in *Math1-cre*/$Ptc^{C/C}$ and *Math1-creER*/$Ptc^{C/C}$ mice, many GNPs are able to differentiate despite loss of *Ptc*, and only a subset of cells continues to proliferate and forms tumors. One explanation for this is that full transformation of GNPs requires changes besides loss of *Ptc*, and these changes only occur in a subset of GNPs. This notion is supported by our studies of conventional $Ptc^{+/-}$ mice (Oliver et al., 2005), which demonstrated that loss of *Ptc* results in preneoplastic lesions but that most of these lesions do not go on to become tumors. Expression profiling of GNPs, preneoplastic cells, and tumor cells suggested that altered expression of genes involved in cell migration, differentiation, or apoptosis might be necessary for complete transformation.

In addition to GNPs, NSCs can also give rise to tumors following deletion of *Ptc*. Loss of *Ptc* in NSCs initially results in expansion of the VZ and increased numbers of stem cells. Our demonstration that *Ptc* deletion causes proliferation of cerebellar stem cells is consistent with previous reports showing a role for Shh in stem cell renewal in other parts of the central nervous system (Ahn and Joyner, 2005; Balordi and Fishell, 2007). Importantly, while *Ptc*-deficient NSCs exhibit increased proliferation, they remain capable of differentiating into astrocytes, oligodendrocytes, and neurons. Indeed, the most dramatic consequences of *Ptc* deletion occur once cells leave the VZ and commit to the granule cell lineage. GNPs in *hGFAP-cre*/$Ptc^{C/C}$ mice undergo rapid expansion, encompass the cerebellum at early postnatal stages, and appear to give rise to medulloblastomas in these mice. Support for this notion comes from the fact that the majority of cells in *hGFAP-cre*/$Ptc^{C/C}$ tumors (like those in *Math1-cre*/$Ptc^{C/C}$ tumors) express GNP markers rather than NSC markers. Moreover, the differentiated cells present within these tumors predominantly express markers of postmitotic granule neurons (NeuN, GABRA6) rather than non-granule neurons, astrocytes, or oligodendrocytes, as would be expected if tumors retained characteristics of multipotent stem cells. The fact that deletion of *Ptc* in NSCs does not lead to other tumor types (e.g., astrocytomas, oligodendrogliomas, or even medulloblastomas with non-GNP characteristics) is remarkable and suggests that the granule lineage may be exquisitely sensitive to the oncogenic effects of hedgehog signaling. Alternatively, it is possible that additional genetic or epigenetic events (besides loss of *Ptc*) are needed for tumor formation and that these are most likely to occur during the rapid expansion of GNPs in the EGL.

While our data suggest that deletion of *Ptc* in *hGFAP*-expressing NSCs does not result in glial tumors, this does not mean that Shh signaling does not play any role in initiation or maintenance of such tumors. For example, it is possible that activation of the hedgehog pathway in distinct progenitors, or in combination with additional oncogenic lesions, might result in formation of astrocytomas or oligodendrogliomas. Moreover, recent studies have suggested that the Shh pathway is active in human glioma and in mouse models of the disease (Becher et al., 2008; Clement et al., 2007; Ehtesham et al., 2007) and that treatment with Shh pathway inhibitors can suppress the growth of glioma cell lines and xenografts (Bar et al., 2007; Clement et al., 2007). These data raise the possibility that Shh signaling, even if it is not involved in tumor initiation, might contribute to tumor growth or maintenance. Further studies of Shh pathway antagonists in transgenic and xenograft models of glioma will be required to determine the importance of this pathway as a therapeutic target.

In the discussion above, we refer to the tumors in *hGFAP-cre*/$Ptc^{C/C}$ mice as being "initiated" in NSCs. Since these tumors do not manifest until cells have committed to the granule lineage, it is reasonable to ask whether they should be more aptly considered to be initiated in GNPs. In this context, we believe it is important to draw a distinction between tumor initiation and transformation. We consider tumor initiation to be the stage at which the first oncogenic mutation occurs, even if this mutation is not sufficient to fully transform the cell. In contrast, we view transformation as the stage at which cells have accumulated all of the oncogenic mutations that they need to form tumors. With this framework in mind, we believe it is appropriate to refer to tumors in *hGFAP-cre*/$Ptc^{C/C}$ mice as initiated in stem cells and to consider NSCs as the cells of origin for these tumors.

In comparing tumors in *hGFAP-cre*/$Ptc^{C/C}$ and *Math1-cre*/$Ptc^{C/C}$ mice, the only marked difference we observed was in tumor latency: *hGFAP-cre*/$Ptc^{C/C}$ mice developed tumors between 3 and 4 weeks of age, whereas *Math1-cre*/$Ptc^{C/C}$ mice developed tumors between 8 and 12 weeks of age. One possible explanation for the rapid expansion of tumors in *hGFAP-cre*/$Ptc^{C/C}$ mice is that deletion of *Ptc* in these animals is more efficient than in *Math1-cre*/$Ptc^{C/C}$ mice and that, as a result, there are more *Ptc*-deficient GNPs to serve as a source for the tumors. However, our analysis suggests that Cre activity (based on induction of GFP in *R26R* reporter mice) and *Ptc* deletion efficiency (based on analysis of genomic *Ptc* levels) are very similar between the two strains. Another possible explanation for the difference in latency is that *hGFAP-cre*/$Ptc^{C/C}$ tumor cells have an increased rate of proliferation or a decreased rate of apoptosis and as a result give rise to more rapidly growing tumors. However, comparison of thymidine incorporation, cell-cycle analysis, caspase activation, and even gene expression did not reveal any significant differences in these parameters between *hGFAP-cre*/$Ptc^{C/C}$ and *Math1-cre*/$Ptc^{C/C}$ tumor cells (Figure 8; unpublished data). Moreover, transplantation of equal numbers of *hGFAP-cre*/$Ptc^{C/C}$ and *Math1-cre*/$Ptc^{C/C}$ tumor cells into immunocompromised mice results in similar tumor latency in recipients.

Thus, intrinsic differences between *hGFAP-cre/Ptc*$^{C/C}$ and *Math1-cre/Ptc*$^{C/C}$ tumor cells are also not likely to account for the differences in age of tumor onset.

Instead, the differences in tumor latency are most likely a consequence of the stage at which *Ptc* deletion occurs. Deletion of *Ptc* in the VZ (using *hGFAP-cre* mice) leads to an early expansion of the stem cell pool. A larger stem cell pool leads, in turn, to a significant increase in the starting number of GNPs, which then continue to expand and ultimately contribute to tumor bulk. Since animals develop symptoms when tumors reach a critical mass, having a larger pool of *Ptc*-deficient GNPs at the outset allows *hGFAP-cre/Ptc*$^{C/C}$ mice to reach this stage much more quickly than *Math1-cre/Ptc*$^{C/C}$ mice. This model may also explain the shorter latency of tumors in *Math1-cre/Ptc*$^{C/C}$ mice compared to *Math1-creER/Ptc*$^{C/C}$ mice that are exposed to tamoxifen postnatally: whereas embryonic deletion of *Ptc* targets all GNPs, postnatal deletion targets only the subset of GNPs that have not yet differentiated. As a result, it takes GNPs in postnatally targeted animals longer to reach critical mass. The same may be true for tumors in other tissues: the earlier in a given lineage that an oncogenic mutation occurs, the more opportunity there is for expansion of cells bearing this mutation, and the more dramatic the consequences for the animal.

These observations may have particular significance for human medulloblastoma. Although medulloblastoma can occur in children as well as adults, patients who develop tumors at a very young age (<3 years) have a high risk for treatment failure and relapse, while those who develop the disease when they are older tend to have a more favorable outcome (Kalifa and Grill, 2005). One reason for this may be that radiation therapy, which is commonly used in older patients, is withheld from young children because it is considered to be too damaging for the developing brain. Thus, tumors in young children may grow faster because they are treated less aggressively. However, our findings suggest that the cell in which the tumor is initiated may also contribute to the age of onset and the difference in prognosis: tumors that occur in young children may arise from mutations in multipotent stem cells, whereas those in older children may originate from more differentiated progenitors. In the former case, as in our *hGFAP-cre/Ptc*$^{C/C}$ mice, expansion of stem cells and increased production of GNPs may contribute to more rapid tumor growth and earlier onset of symptoms.

Identifying the cell of origin for medulloblastoma may also have important implications for therapy. Recent studies have shown that many brain tumors contain NSC-like cells and have suggested that these cells are important for tumor propagation (Hemmati et al., 2003; Singh et al., 2004). In light of this, many investigators have begun to develop targeted therapies to eradicate such cells. Our studies demonstrate that not all brain tumors are derived from cells with a stem cell phenotype. In particular, we show that Shh pathway-associated medulloblastomas may be initiated in either progenitors or stem cells and ultimately adopt a phenotype that resembles GNPs rather than NSCs. Whether the same is true for other subtypes of medulloblastoma remains to be investigated. Determining whether a tumor is derived from lineage-restricted progenitors or stem cells, finding markers specific for these cells, and identifying signals that control their growth and differentiation may be important prerequisites for effective therapy.

EXPERIMENTAL PROCEDURES

Mice

Ptc$^{C/C}$ mice and *Math1-creER* mice have been described previously (Ellis et al., 2003; Machold and Fishell, 2005). *hGFAP-GFP* mice (Zhuo et al., 1997), *hGFAP-cre* mice (Zhuo et al., 2001), and *R26R-GFP* reporter mice (Mao et al., 2001) were from The Jackson Laboratory. SCID/beige mice were from Charles River Laboratories. Animals were maintained in the Cancer Center Isolation Facility at Duke University, and all experiments were performed in accordance with procedures approved by the Duke University Animal Care and Use Committee.

Histology and Immunohistochemistry

For histological analysis, animals were perfused with PBS followed by 4% paraformaldehyde (PFA). Cerebella were removed, fixed in 4% PFA overnight, transferred to 70% ethanol and embedded in paraffin. Sections (5 μm) were stained with hematoxylin and eosin (Sigma) or with anti-BrdU or anti-group B1 Sox antibodies (Tanaka et al., 2004).

For immunohistochemistry, cerebella from PFA-perfused animals were fixed overnight in 4% PFA, cryoprotected in 30% sucrose, frozen in Tissue Tek-OCT (Sakura Finetek), and cut into 10–12 μm sagittal sections. Sections were blocked and permeabilized for 2 hr with PBS containing 0.1% Triton X-100 and 1% normal goat serum, stained with primary antibodies overnight at 4°C, and incubated with secondary antibodies for 2 hr at room temperature. Sections were counterstained with DAPI and mounted with Fluoromount-G (Southern Biotech) before being visualized using a Nikon TE200 microscope. Antibodies used for immunostaining are listed in Supplemental Experimental Procedures.

Cell Isolation and Proliferation Assays

Cerebella from P6 mice were digested with 10 U/ml papain (Worthington Biochemical), 200 μg/ml L-cysteine, and 250 U/ml DNase (Sigma); triturated to obtain a single-cell suspension; and then centrifuged through a 35%–65% Percoll gradient (Sigma). Cells from the 35%–65% interface were suspended in NB-B27 (Neurobasal with 1 mM sodium pyruvate, 2 mM L-glutamine, penicillin/streptomycin, and B27 supplement, all from Invitrogen) and transferred to poly-D-lysine-coated 96-well plates at a density of 2×10^5 cells per well. After 48 hr, cells were pulsed with [methyl-^{3}H]thymidine (Amersham/GE Healthcare) and cultured for an additional 16–18 hr. Cells were harvested onto filters using a Mach IIIM Manual Harvester 96 (Tomtec), and incorporated radioactivity was quantified by liquid scintillation spectrophotometry on a Wallac MicroBeta scintillation counter (PerkinElmer).

Laser Capture Microdissection and Real-Time RT-PCR

Cerebella were removed immediately and frozen in OCT. Sagittal sections (5 μm) were mounted onto glass slides, fixed in 75% ethanol for 30 s, and stained with cresyl violet (Ambion). After 5 min of air drying, microdissection was carried out using a PixCell IIe LCM system (Arcturus Bioscience). RNA was extracted from LCM caps using an RNA isolation kit (Arcturus Bioscience). For real-time RT-PCR, first-strand cDNA was synthesized from equal amounts of RNA (0.1–1 μg) using SuperScript III Reverse Transcriptase (Invitrogen). Triplicate reactions were prepared using a 25 μl mixture containing iQ SYBR Green Supermix (Bio-Rad). Real-time quantification was performed on a Bio-Rad iCycler iQ system. Serial 10-fold dilutions of cDNA were used as references for the standard curve. Raw data were normalized based on expression of actin. Primers used for *Gli1*, N-*myc*, *Cyclin D1*, and *Ptc* are listed in Supplemental Experimental Procedures.

Intracranial Transplantation

SCID/beige mice (6–8 weeks old) were anesthetized with xylazine (25 mg/kg, Lloyd Laboratories) and ketamine (125 mg/kg, Fort Dodge Animal Health) and placed in a stereotaxic apparatus (David Kopf Instruments). After exposing the skull with a scalpel, a 1 mm diameter hole was drilled in the skull over the cerebellum using an 18G needle. A cell suspension (1×10^6 cells in 5 μl NB-B27) was slowly injected into the cerebellum at a depth of 1 mm using a 5 μl Hamilton syringe with an unbeveled 24G needle. After injection, the incision was sutured using catgut sutures (Johnson & Johnson).

Tamoxifen Treatment

Tamoxifen (T5648, Sigma) was prepared as a 20 mg/ml stock solution in corn oil (Sigma). Tamoxifen was administered by oral gavage using 24G gavaging needles (Fine Science Tools). Tamoxifen doses were 0.6 mg/30 μl at P4, 1 mg/50 μl at P8, 1.4 mg/70 μl at P10, 1.6 mg/80 μl at P12, and 4.0 mg/200μl for treatment of pregnant females.

Neurosphere Cultures

To generate primary neurospheres, cells from E14.5 embryonic cerebella were plated at 2 × 10^5 cells/ml in NSC proliferation medium (NeuroCult basal medium with proliferation supplement, Stem Cell Technologies) plus 10 ng/ml basic fibroblast growth factor and 20 ng/ml epidermal growth factor (PeproTech). Neurospheres were counted or harvested for immunostaining after 7 days in culture. For self-renewal assays, neurospheres were mechanically dissociated and replated in fresh proliferation medium at 2 × 10^3 cells/ml. For differentiation assays, neurospheres were plated on poly-D-lysine-coated coverslips (BD Biosciences) in NSC differentiation medium (NeuroCult basal medium with differentiation supplement). Seven days after plating, cultures were fixed with 4% PFA for immunostaining.

SUPPLEMENTAL DATA

The Supplemental Data include Supplemental Experimental Procedures, one table, and eight figures and can be found with this article online at http://www.cancercell.org/cgi/content/full/14/2/135/DC1/.

ACKNOWLEDGMENTS

The authors thank Susan Su, Pate Skene, and the NIH Neuroscience Microarray Consortium for help with laser capture and microarray analysis; Simon Lin at Northwestern University for assistance with bioinformatics; Beth Harvat and Mike Cook for flow cytometry; and Jack Dutton, Mark Johnson, and Zhen Zhao for assistance with animal colony maintenance. T.E. is a John Trivett Senior Research Fellow. This work was supported by funds from the National Health and Medical Research Council of Australia (B.J.W.), the ARC Special Research Centre for Functional and Applied Genomics (B.J.W.), the Queensland Cancer Fund (B.J.W.), the Hope Street Kids Foundation (Z.-J.Y.), the Kislak-Sussman Fund (R.J.W.-R.), the Children's Brain Tumor Foundation (R.J.W.-R.), the Pediatric Brain Tumor Foundation (R.J.W.-R.), the McDonnell Foundation (R.J.W.-R.), the Australian Cancer Research Foundation, and NINDS grant number NS052323-01 (R.J.W.-R.).

Received: February 2, 2008
Revised: June 4, 2008
Accepted: July 7, 2008
Published: August 11, 2008

REFERENCES

Adolphe, C., Hetherington, R., Ellis, T., and Wainwright, B. (2006). Patched1 functions as a gatekeeper by promoting cell cycle progression. Cancer Res. *66*, 2081–2088.

Ahn, S., and Joyner, A.L. (2005). In vivo analysis of quiescent adult neural stem cells responding to Sonic hedgehog. Nature *437*, 894–897.

Balordi, F., and Fishell, G. (2007). Hedgehog signaling in the subventricular zone is required for both the maintenance of stem cells and the migration of newborn neurons. J. Neurosci. *27*, 5936–5947.

Bar, E.E., Chaudhry, A., Lin, A., Fan, X., Schreck, K., Matsui, W., Piccirillo, S., Vescovi, A.L., DiMeco, F., Olivi, A., and Eberhart, C.G. (2007). Cyclopamine-mediated hedgehog pathway inhibition depletes stem-like cancer cells in glioblastoma. Stem Cells *25*, 2524–2533.

Becher, O.J., Hambardzumyan, D., Fomchenko, E.I., Momota, H., Mainwaring, L., Bleau, A.M., Katz, A.M., Edgar, M., Kenney, A.M., Cordon-Cardo, C., et al. (2008). Gli activity correlates with tumor grade in platelet-derived growth factor-induced gliomas. Cancer Res. *68*, 2241–2249.

Buhren, J., Christoph, A.H., Buslei, R., Albrecht, S., Wiestler, O.D., and Pietsch, T. (2000). Expression of the neurotrophin receptor p75NTR in medulloblastomas is correlated with distinct histological and clinical features: evidence for a medulloblastoma subtype derived from the external granule cell layer. J. Neuropathol. Exp. Neurol. *59*, 229–240.

Casper, K.B., and McCarthy, K.D. (2006). GFAP-positive progenitor cells produce neurons and oligodendrocytes throughout the CNS. Mol. Cell. Neurosci. *31*, 676–684.

Clement, V., Sanchez, P., de Tribolet, N., Radovanovic, I., and Ruiz i Altaba, A. (2007). HEDGEHOG-GLI1 signaling regulates human glioma growth, cancer stem cell self-renewal, and tumorigenicity. Curr. Biol. *17*, 165–172.

Cozzio, A., Passegue, E., Ayton, P.M., Karsunky, H., Cleary, M.L., and Weissman, I.L. (2003). Similar MLL-associated leukemias arising from self-renewing stem cells and short-lived myeloid progenitors. Genes Dev. *17*, 3029–3035.

Eberhart, C.G. (2007). In search of the medulloblast: neural stem cells and embryonal brain tumors. Neurosurg. Clin. N. Am. *18*, 59–69.

Ehtesham, M., Sarangi, A., Valadez, J.G., Chanthaphaychith, S., Becher, M.W., Abel, T.W., Thompson, R.C., and Cooper, M.K. (2007). Ligand-dependent activation of the hedgehog pathway in glioma progenitor cells. Oncogene *26*, 5752–5761.

Ellis, T., Smyth, I., Riley, E., Graham, S., Elliot, K., Narang, M., Kay, G.F., Wicking, C., and Wainwright, B. (2003). Patched 1 conditional null allele in mice. Genesis *36*, 158–161.

Ellison, D. (2002). Classifying the medulloblastoma: insights from morphology and molecular genetics. Neuropathol. Appl. Neurobiol. *28*, 257–282.

Gilbertson, R.J., and Ellison, D.W. (2008). The origins of medulloblastoma subtypes. Annu. Rev. Pathol. *3*, 341–365.

Goodrich, L.V., Johnson, R.L., Milenkovic, L., McMahon, J.A., and Scott, M.P. (1996). Conservation of the hedgehog/patched signaling pathway from flies to mice: induction of a mouse patched gene by Hedgehog. Genes Dev. *10*, 301–312.

Goodrich, L.V., Milenkovic, L., Higgins, K.M., and Scott, M.P. (1997). Altered neural cell fates and medulloblastoma in mouse *patched* mutants. Science *277*, 1109–1113.

Hahn, H., Wicking, C., Zaphiropoulous, P.G., Gailani, M.R., Shanley, S., Chidambaram, A., Vorechovsky, I., Holmberg, E., Unden, A.B., Gillies, S., et al. (1996). Mutations of the human homolog of Drosophila patched in the nevoid basal cell carcinoma syndrome. Cell *85*, 841–851.

Hahn, H., Wojnowski, L., Specht, K., Kappler, R., Calzada-Wack, J., Potter, D., Zimmer, A., Muller, U., Samson, E., and Quintanilla-Martinez, L. (2000). Patched target Igf2 is indispensable for the formation of medulloblastoma and rhabdomyosarcoma. J. Biol. Chem. *275*, 28341–28344.

Hamre, K.M., and Goldowitz, D. (1997). meander tail acts intrinsic to granule cell precursors to disrupt cerebellar development: analysis of meander tail chimeric mice. Development *124*, 4201–4212.

Hashimoto, M., and Mikoshiba, K. (2003). Mediolateral compartmentalization of the cerebellum is determined on the "birth date" of Purkinje cells. J. Neurosci. *23*, 11342–11351.

Heikens, J., Michiels, E.M., Behrendt, H., Endert, E., Bakker, P.J., and Fliers, E. (1998). Long-term neuro-endocrine sequelae after treatment for childhood medulloblastoma. Eur. J. Cancer *34*, 1592–1597.

Hemmati, H.D., Nakano, I., Lazareff, J.A., Masterman-Smith, M., Geschwind, D.H., Bronner-Fraser, M., and Kornblum, H.I. (2003). Cancerous stem cells can arise from pediatric brain tumors. Proc. Natl. Acad. Sci. USA *100*, 15178–15183.

Johnson, R.L., Rothman, A.L., Xie, J., Goodrich, L.V., Bare, J.W., Bonifas, J.M., Quinn, A.G., Myers, R.M., Cox, D.R., Epstein, E.H., Jr., and Scott, M.P. (1996). Human homolog of patched, a candidate gene for the basal cell nevus syndrome. Science *272*, 1668–1671.

Kalifa, C., and Grill, J. (2005). The therapy of infantile malignant brain tumors: current status? J. Neurooncol. *75*, 279–285.

Kenney, A.M., Cole, M.D., and Rowitch, D.H. (2003). Nmyc upregulation by sonic hedgehog signaling promotes proliferation in developing cerebellar granule neuron precursors. Development *130*, 15–28.

Krivtsov, A.V., Twomey, D., Feng, Z., Stubbs, M.C., Wang, Y., Faber, J., Levine, J.E., Wang, J., Hahn, W.C., Gilliland, D.G., et al. (2006). Transformation

from committed progenitor to leukaemia stem cell initiated by MLL-AF9. Nature *442*, 818–822.

Machold, R., and Fishell, G. (2005). Math1 is expressed in temporally discrete pools of cerebellar rhombic-lip neural progenitors. Neuron *48*, 17–24.

Mao, X., Fujiwara, Y., Chapdelaine, A., Yang, H., and Orkin, S.H. (2001). Activation of EGFP expression by Cre-mediated excision in a new ROSA26 reporter mouse strain. Blood *97*, 324–326.

Mulhern, R.K., Palmer, S.L., Merchant, T.E., Wallace, D., Kocak, M., Brouwers, P., Krull, K., Chintagumpala, M., Stargatt, R., Ashley, D.M., et al. (2005). Neurocognitive consequences of risk-adapted therapy for childhood medulloblastoma. J. Clin. Oncol. *23*, 5511–5519.

Oliver, T.G., Grasfeder, L.L., Carroll, A.L., Kaiser, C., Gillingham, C.L., Lin, S.M., Wickramasinghe, R., Scott, M.P., and Wechsler-Reya, R.J. (2003). Transcriptional profiling of the Sonic hedgehog response: a critical role for N-myc in proliferation of neuronal precursors. Proc. Natl. Acad. Sci. USA *100*, 7331–7336.

Oliver, T.G., Read, T.A., Kessler, J.D., Mehmeti, A., Wells, J.F., Huynh, T.T., Lin, S.M., and Wechsler-Reya, R.J. (2005). Loss of patched and disruption of granule cell development in a pre-neoplastic stage of medulloblastoma. Development *132*, 2425–2439.

Packer, R.J., Cogen, P., Vezina, G., and Rorke, L.B. (1999). Medulloblastoma: clinical and biologic aspects. Neuro-oncol. *1*, 232–250.

Pevny, L., and Placzek, M. (2005). SOX genes and neural progenitor identity. Curr. Opin. Neurobiol. *15*, 7–13.

Pomeroy, S.L., Sutton, M.E., Goumnerova, L.C., and Segal, R.A. (1997). Neurotrophins in cerebellar granule cell development and medulloblastoma. J. Neurooncol. *35*, 347–352.

Raffel, C., Jenkins, R.B., Frederick, L., Hebrink, D., Alderete, B., Fults, D.W., and James, C.D. (1997). Sporadic medulloblastomas contain PTCH mutations. Cancer Res. *57*, 842–845.

Read, T.A., Hegedus, B., Wechsler-Reya, R., and Gutmann, D.H. (2006). The neurobiology of neurooncology. Ann. Neurol. *60*, 3–11.

Romer, J.T., Kimura, H., Magdaleno, S., Sasai, K., Fuller, C., Baines, H., Connelly, M., Stewart, C.F., Gould, S., Rubin, L.L., and Curran, T. (2004). Suppression of the Shh pathway using a small molecule inhibitor eliminates medulloblastoma in Ptc1(+/−)p53(−/−) mice. Cancer Cell *6*, 229–240.

Salsano, E., Pollo, B., Eoli, M., Giordana, M.T., and Finocchiaro, G. (2004). Expression of MATH1, a marker of cerebellar granule cell progenitors, identifies different medulloblastoma sub-types. Neurosci. Lett. *370*, 180–185.

Sanchez, P., and Ruiz i Altaba, A. (2005). In vivo inhibition of endogenous brain tumors through systemic interference of Hedgehog signaling in mice. Mech. Dev. *122*, 223–230.

Schüller, U., Zhao, Q., Godinho, S.A., Heine, V.M., Medema, R.H., Pellman, D., and Rowitch, D.H. (2007). Forkhead transcription factor FoxM1 regulates mitotic entry and prevents spindle defects in cerebellar granule neuron precursors. Mol. Cell. Biol. *27*, 8259–8270.

Singh, S.K., Clarke, I.D., Terasaki, M., Bonn, V.E., Hawkins, C., Squire, J., and Dirks, P.B. (2003). Identification of a cancer stem cell in human brain tumors. Cancer Res. *63*, 5821–5828.

Singh, S.K., Hawkins, C., Clarke, I.D., Squire, J.A., Bayani, J., Hide, T., Henkelman, R.M., Cusimano, M.D., and Dirks, P.B. (2004). Identification of human brain tumour initiating cells. Nature *432*, 396–401.

Spassky, N., Han, Y.G., Aguilar, A., Strehl, L., Besse, L., Laclef, C., Romaguera Ros, M., Garcia-Verdugo, J.M., and Alvarez-Buylla, A. (2008). Primary cilia are required for cerebellar development and Shh-dependent expansion of progenitor pool. Dev. Biol. *317*, 246–259.

Surmeier, D.J., Mermelstein, P.G., and Goldowitz, D. (1996). The weaver mutation of GIRK2 results in a loss of inwardly rectifying K+ current in cerebellar granule cells. Proc. Natl. Acad. Sci. USA *93*, 11191–11195.

Tanaka, S., Kamachi, Y., Tanouchi, A., Hamada, H., Jing, N., and Kondoh, H. (2004). Interplay of SOX and POU factors in regulation of the Nestin gene in neural primordial cells. Mol. Cell. Biol. *24*, 8834–8846.

Wang, V.Y., Rose, M.F., and Zoghbi, H.Y. (2005). Math1 expression redefines the rhombic lip derivatives and reveals novel lineages within the brainstem and cerebellum. Neuron *48*, 31–43.

Wechsler-Reya, R.J., and Scott, M.P. (1999). Control of neuronal precursor proliferation in the cerebellum by Sonic Hedgehog. Neuron *22*, 103–114.

Wetmore, C., Eberhart, D.E., and Curran, T. (2001). Loss of p53 but not ARF accelerates medulloblastoma in mice heterozygous for patched. Cancer Res. *61*, 513–516.

Yokota, N., Aruga, J., Takai, S., Yamada, K., Hamazaki, M., Iwase, T., Sugimura, H., and Mikoshiba, K. (1996). Predominant expression of human zic in cerebellar granule cell lineage and medulloblastoma. Cancer Res. *56*, 377–383.

Zhuo, L., Sun, B., Zhang, C.L., Fine, A., Chiu, S.Y., and Messing, A. (1997). Live astrocytes visualized by green fluorescent protein in transgenic mice. Dev. Biol. *187*, 36–42.

Zhuo, L., Theis, M., Alvarez-Maya, I., Brenner, M., Willecke, K., and Messing, A. (2001). hGFAP-cre transgenic mice for manipulation of glial and neuronal function in vivo. Genesis *31*, 85–94.

Zindy, F., Uziel, T., Ayrault, O., Calabrese, C., Valentine, M., Rehg, J.E., Gilbertson, R.J., Sherr, C.J., and Roussel, M.F. (2007). Genetic alterations in mouse medulloblastomas and generation of tumors de novo from primary cerebellar granule neuron precursors. Cancer Res. *67*, 2676–2684.